INTERNATIONAL JOURNAL FOR NUMERICAL METHODS IN FLUIDS, VOL. 14, 1245–1257 (1992)

# CONSERVATIVE MONOTONE STREAMLINE UPWIND FORMULATION USING SIMPLEX ELEMENTS

F. SHEMIRANI AND K. JAMBUNATHAN

*Department of Mechanical Engineering, Faculty of Engineering, Nottingham Polytechnic, Nottingham NG1 4BU, U.K.*

SUMMARY

A streamline upwind formulation is presented for the treatment of the advection terms in the general transport equation. The formulation is monotone and conservative and is based on the discontinuous nature of the advection mechanism. The results of three benchmark test cases for the full range of flow Peclet numbers are presented. The new formulation is shown to accurately model the advection phenomenon with significantly smaller numerical diffusion than the existing methods. The results are also free of all spatial oscillations. Considerable savings in computer storage and execution time have been achieved by employing the three-noded triangular element for which exact integrations exist. The formulation is straightforward and can be readily incorporated into any finite element code using the conventional Galerkin approach.

KEY WORDS Advection modelling Streamline upwind Finite element

## 1. INTRODUCTION

The numerical treatment of the advection phenomenon is still attracting considerable research interest. Numerical modellers are constantly looking for more stable, accurate and efficient approximations to the first-order non-linear advective terms in the general transport equation. Initial attempts to treat such terms by central difference operators in the finite difference method (FDM) resulted in spurious oscillations for cases with grid Peclet numbers greater than 2·0. This shortcoming has, to varying degrees, been alleviated by the use of the exponential and hybrid schemes,[1] the power-law scheme,[2] the higher-order upwind differencing (HOU) scheme,[3,4] the quadratic upwind (QUICK) scheme[5] and the streamline upwind scheme.[6] Unfortunately, all these schemes and their variants produce numerical diffusion and/or spatial oscillations to varying extents. Advection modelling continues to remain one of the central issues in the FDM.[7]

The finite element method (FEM) is experiencing similar difficulties. The conventional Galerkin weighted residual approach, akin to the central difference operator, produces unacceptable levels of numerical diffusion and spatial oscillations. The streamline upwind/Petrov–Galerkin (SUPG) scheme,[8,9] with good stability properties, dampens the numerical dispersion and results in faster convergence rates than the other upwind methods. The levels of spatial oscillations produced by SUPG, however, means its exclusion from applications where boundary and internal layers are present. More stable solutions may be obtained by the use of monotone methods.[10,11] These methods, however, generally violate the conservation laws, resulting in global imbalance of the transported quantities. Discontinuity-capturing versions of SUPG[12–15] have been implemented for multidimensional situations to give improved stability. However, this is only attainable at the expense of the cross-wind diffusion reappearing in the final solution.

0271–2091/92/101245–13$06.50

*Received November 1990*
*Revised October 1991*

Nevertheless, the FEM generally produces less numerical diffusion than the FDM[16,17] owing to the fact that the former can operate in the resultant velocity direction as opposed to the locally one-dimensional approach usually adopted in the FDM.

In this paper we have reverted to monotone techniques because of their simplicity, efficiency and ease with which they can be implemented in multidimensional situations. In particular, close examination of the monotone streamline upwind (MSU) approximation[11] reveals that a conservative form of the method could be developed for simplex triangular elements. The original non-conservative MSU was developed in conjunction with bilinear rectangular elements. For purely diffusive problems these elements, depending on their aspect ratios, may lead to a non-diagonally dominant global coefficient matrix. This in turn prohibits the use of iterative solvers, which are much more efficient than their direct counterparts. The simplex elements on the other hand, owing to their shape function properties, will result in diagonally dominant global coefficient matrices. Also, exact integrations can be used for simplex elements, which reduce the computer storage and run time requirements. Furthermore, complete triangularization of any arbitrary domain in space is possible.

The detailed derivation of the current formulation and its application to three benchmark test cases are presented in the rest of this paper. The results show minimum levels of numerical diffusion in the absence of spatial oscillations across the entire flow Peclet number range.

## 2. CONSERVATIVE MONOTONE STREAMLINE UPWIND FORMULATION

Here only the two-dimensional form of the formulation is presented. Its extension to three dimensions will be carried out in the near future. The conservative form of the general steady state transport equation for a scalar quantity $\phi$ in two-dimensional Cartesian co-ordinates (with the usual notation) is

$$\frac{\partial}{\partial x}(\rho u\phi)+\frac{\partial}{\partial y}(\rho v\phi)=\frac{\partial}{\partial x}\left(\Gamma_\phi\frac{\partial\phi}{\partial x}\right)+\frac{\partial}{\partial y}\left(\Gamma_\phi\frac{\partial\phi}{\partial y}\right)+S_\phi. \tag{1}$$

In solving the above equation, a known velocity field was assumed to have been established. The finite element discretization begins by subdividing the domain of interest into three-noded triangular elements as shown in Figure 1. Variations in $\phi$ within the element are described by

$$\phi = L_i\phi_i + L_j\phi_j + L_k\phi_k, \qquad L_i + L_j + L_k = 0. \tag{2}$$

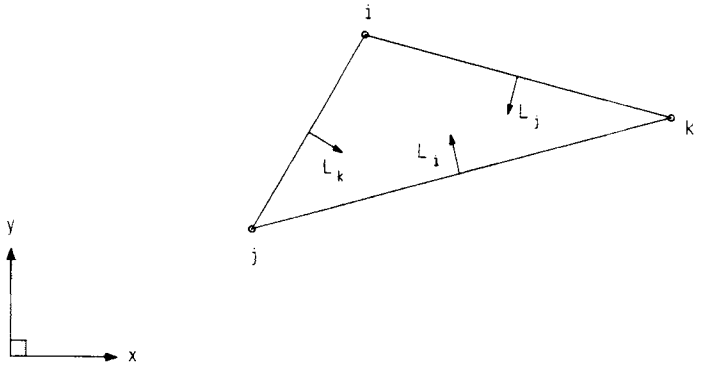


Figure 1. Simplex elements with natural co-ordinates

At the elemental level equation (1) is weighted and integrated over the element area; hence

$$\int_{A^e} N\left(\frac{\partial}{\partial x}(\rho u\phi)+\frac{\partial}{\partial y}(\rho v\phi)\right)\mathrm{d}A^e=\int_{A^e} N\left[\frac{\partial}{\partial x}\left(\Gamma_\phi\frac{\partial\phi}{\partial x}\right)+\frac{\partial}{\partial y}\left(\Gamma_\phi\frac{\partial\phi}{\partial y}\right)+S_\phi\right]\mathrm{d}A^e. \tag{3}$$

The diffusion and source terms are treated by the conventional Galerkin weighted residual approach.[18] The treatment of the advection terms, which is the subject of this paper, can be demonstrated by rewriting equation (3) as

$$\int_{A^e} N\left(\frac{\partial}{\partial x}(\rho u\phi)+\frac{\partial}{\partial y}(\rho v\phi)\right)\mathrm{d}A^e=\text{constant}, \tag{4}$$

where the constant on the right-hand side is due to the combined effect of the diffusion and source terms. Expressing the above equation in terms of the streamline co-ordinates shown in Figure 2,

$$\int_{A^e} N\left(\frac{\partial}{\partial s}(\rho u_s\phi)\right)\mathrm{d}A^e=\text{constant}, \tag{5}$$

where the two-dimensional advection problem in equation (4) is now reduced to a one-dimensional equation describing the local derivative of $\rho u_s\phi$ along the segment of a streamline contained within an element, with $s$ being the tangential streamline co-ordinate. Equation (5) states that in the absence of the diffusion and source terms, the quantity $\rho u_s\phi$ is transported unchanged along the streamline segment from an upstream point to downstream locations. This is an important observation and one that is reflected in the present formulation. To evaluate the above integral, it is first assumed that within an element

$$\frac{\partial}{\partial s}(\rho u_s\phi)=\text{constant}. \tag{6}$$

Note that for the special case of pure advection the constant in the above equation is equal to zero. Using equation (6), equation (5) can now be simplified to

$$\frac{\partial}{\partial s}(\rho u_s\phi)\int_{A^e} N\,\mathrm{d}A^e=\frac{\partial}{\partial s}(\rho u_s\phi)\,A_f=\text{constant}, \tag{7}$$

where $A_f$ is the sum of shape function integrals of elements surrounding a node. The derivative term in equation (7) is evaluated by considering the streamlines passing through an element positioned in the flow field as illustrated in Figure 3. As shown in this figure, node $i$ is a 'downwind' node for which the negative of the velocity vector $u_{si}$ points back into the element. For any element there are four possible streamline–element configurations as illustrated in

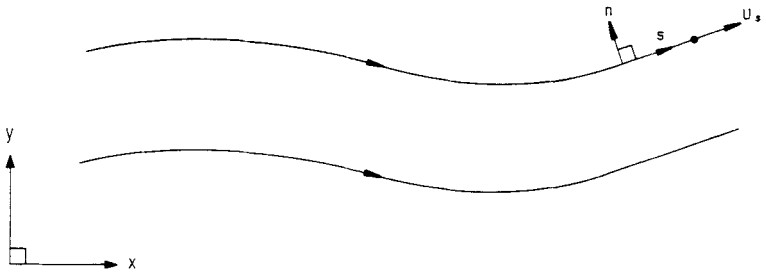


Figure 2. Streamline co-ordinates

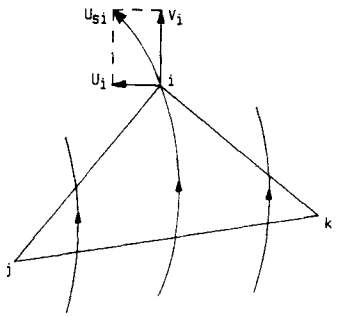


Figure 3. Downwind node illustration

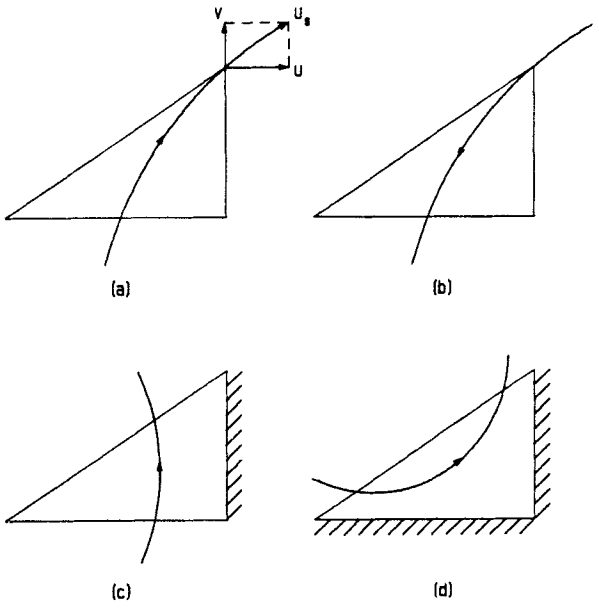


Figure 4. Possible streamline–element configurations: (a) one downwind node; (b)–(d) no downwind nodes

Figure 4. For elements situated in the core of the flow (Figures 4(a) and 4(b)) there may exist one, and only one, downwind node (Figure 4(a)). For elements with one or two sides lying along the solid boundaries (Figures 4(c) and 4(d)) no such downwind node exists. As shown in Figure 5, on a given element a downwind node is identified by

$$u_i \Delta y_{ik} - v_i \Delta x_{ik} \geqslant 0, \qquad u_i \Delta y_{ij} - v_i \Delta x_{ij} \geqslant 0. \tag{8}$$

Once a downwind node has been identified, the interception of the streamline passing through that node with the opposite side is located. As shown in Figure 6, this interception takes place on side $jk$ at the 'upstream' location with co-ordinates $x'$ and $y'$, which are calculated by employing the interpolation factor $F_p$ expressed as

$$F_p = \tfrac{1}{2}(F'_p + F''_p). \tag{9}$$

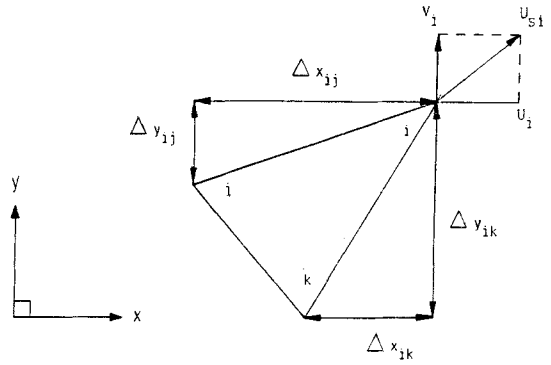


Figure 5. Downwind node identification

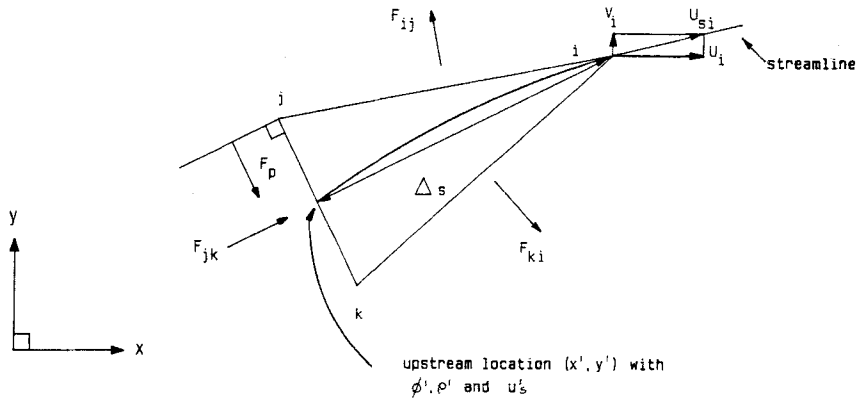


Figure 6. Determination of upstream location

Here $F'_p$ and $F''_p$ are obtained by considering the normal mass flow rates across the element sides, i.e. with reference to Figure 6

$$F'_p = \text{Max}\left\{\text{Min}\left\{\frac{F_{ij}}{F_{jk}}, 1\right\}, 0\right\}, \qquad F''_p = 1 - \text{Max}\left\{\text{Min}\left\{\frac{F_{ki}}{F_{jk}}, 1\right\}, 0\right\}, \tag{10}$$

where

$$F_{ij} = \int_i^j -\rho v\,\mathrm{d}x + \int_i^j \rho u\,\mathrm{d}y, \qquad F_{jk} = -\left(\int_j^k -\rho v\,\mathrm{d}x + \int_j^k \rho u\,\mathrm{d}y\right),$$
$$F_{ki} = \int_k^i -\rho v\,\mathrm{d}x + \int_k^i \rho u\,\mathrm{d}y. \tag{11}$$

It is seen from equations (9) and (10) that $F_p$ is made to vary between zero and unity in order to locate the upstream point along side $jk$. In Figure 6 $x'$ and $y'$ are calculated as

$$x' = (1 - F_p)x_j + F_p x_k, \qquad y' = (1 - F_p)y_j + F_p y_k. \tag{12}$$

Hence the upstream location coincides with node $j$ when $F_p = 0$ and with node $k$ when $F_p = 1$. For values of $F_p$ between zero and unity the upstream location would lie somewhere along side $jk$ between nodes $j$ and $k$. Other element variables at the upstream location can also be calculated in a similar fashion:

$$\phi' = (1 - F_p)\phi_j + F_p\phi_k, \qquad \rho' = (1 - F_p)\rho_j + F_p\rho_k, \qquad u'_s = (1 - F_p)u_{sj} + F_p u_{sk}. \tag{13}$$

With the above definitions, the advection integral (equation (7)) for the element shown in Figure 6 is finally approximated to

$$\frac{\partial}{\partial s}(\rho u_s \phi) A_f \simeq \frac{\rho_i u_{si}\phi_i - \rho' u'_s \phi'}{\Delta s} A_f, \tag{14}$$

with

$$\Delta s = [(x_i - x')^2 + (y_i - y')^2]^{1/2}. \tag{15}$$

In equation (14) the derivative term is approximated conservatively by simply assuming the quantity $\rho u \phi$ to vary linearly along the streamline segment within the element. Alternatively, this approximation can be performed more accurately by considering $\rho$, $u$ and $\phi$ to each vary linearly along the streamline segment. For the test cases that are considered in this paper, the latter made negligible changes to the final results. However, it must be noted that for flow cases where steep gradients in the fluid properties may exist, or where only a limited number of elements can be used, the latter approximation may prove necessary. Also, as can be seen from the above formulation, determination of the upstream location, although it accounts for the streamline curvature within the element, evaluates the length of the streamline segment $\Delta s$ as a straight line. The original MSU[11] considers this point and the authors express negligible gain when using a quadratic arc as opposed to the straight line.

With equations (14) and (15) the advection contribution to the element coefficient matrix can now be constructed. Table I shows the coefficient matrix arising from pure advection for the element shown in Figure 6. Note that the current formulation ensures a diagonally dominant element coefficient matrix, irrespective of the element size and orientation and regardless of the flow Peclet number. The global coefficient matrix may now be assembled by considering the contributions of all elements.

Table I. Element coefficient matrix for pure advection

| row \ column | i | j | k |
|---|---|---|---|
| i | $\frac{\rho_i u_{si}}{\Delta s} A_f$ | $-(1-F_p)\frac{\rho' u'_s}{\Delta s} A_f$ | $-F_p \frac{\rho' u'_s}{\Delta s} A_f$ |
| j | 0 | 0 | 0 |
| k | 0 | 0 | 0 |

## 3. TEST CASE RESULTS

### 3.1. *Pure advection skew to mesh*

This test case has been commonly employed to examine candidate techniques for the treatment of the advection terms.[8,11,12,19–21] The flow domain together with the boundary conditions are shown in Figure 7. The variation in $\phi$ along the exit plane ($0 < S < 2$) is investigated for the case of pure advection ($Pe = \infty$) for three flow angles, $\theta = 22{\cdot}5°$, $45°$ and $67{\cdot}5°$. To be consistent with previous works, the domain is subdivided into 11 equally spaced rows and columns, resulting in a regular mesh with 121 nodes and 200 elements as shown in Figure 8. The exact solution to this problem is determined by advecting the upwind boundary conditions to the exit plane, taking into account the linear interpolation of $\phi$ between the nodes.

Figures 9(a)–9(c) show the results of the current work in comparison with previously published results. It is seen that the current formulation exhibits no spatial oscillations and shows the least

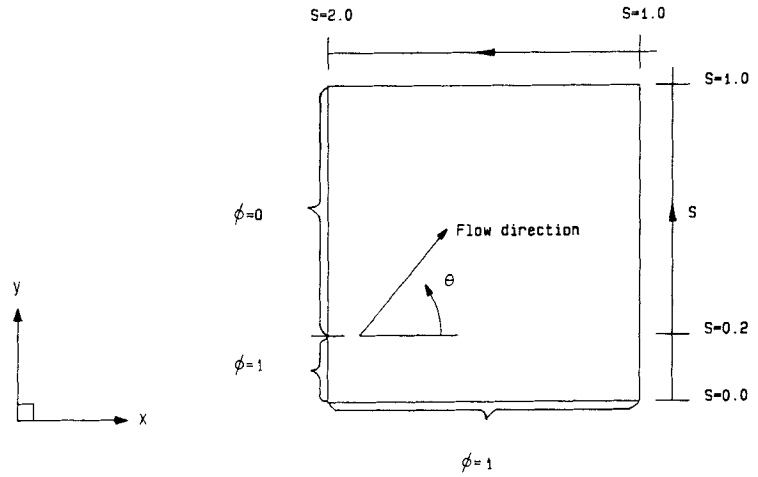


Figure 7. Pure advection skew to mesh

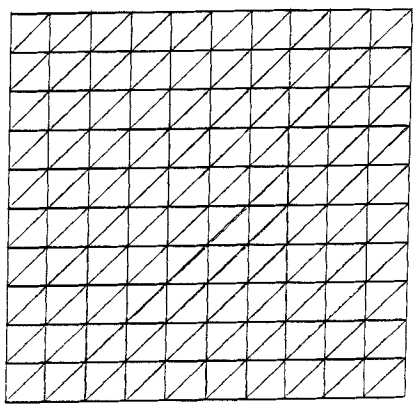

Figure 8. Computational grid for pure advection skew to mesh

false diffusion. For $\theta = 45°$ the formulation follows the exact solution. General superiority of the current formulation over the conventional Galerkin and upwind techniques is also apparent. The percentage false diffusion is calculated as

$$\text{Percentage false diffusion} = \left| \frac{\phi_{\text{exact}} - \phi_{\text{predicted}}}{\phi_{\text{maximum}}} \right| \times 100\%. \tag{16}$$

The current formulation produces maximum false diffusion of 35%, 0% and 35% at flow angles

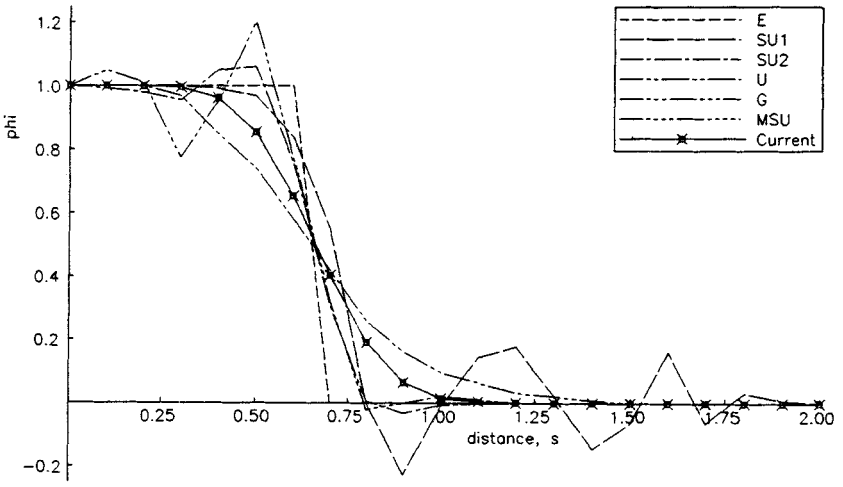


(a)

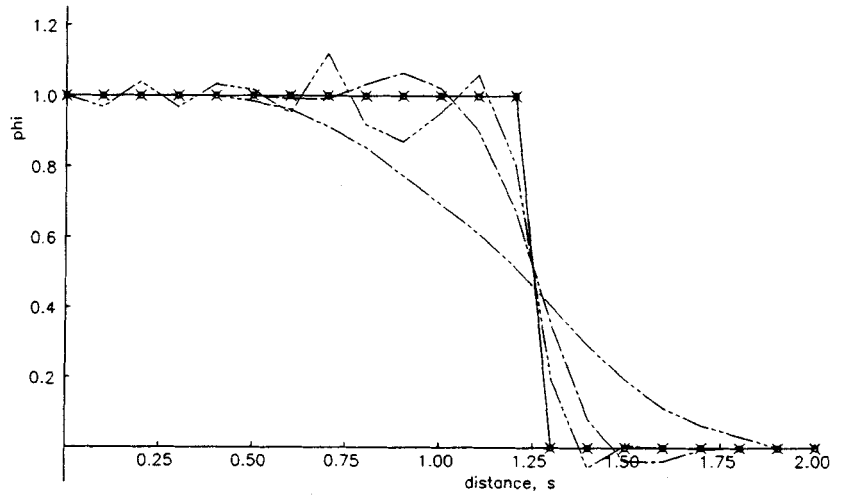


(b)

Figure 9. Comparison of results for pure advection skew to mesh: E, exact; SU1, streamline upwind;[8] SU2, streamline upwind;[8] U, standard upwind;[22] G, Galerkin; MSU, monotone streamline upwind;[11] $\theta$=(a) 22·5°, (b) 45°, (c) 67·5°

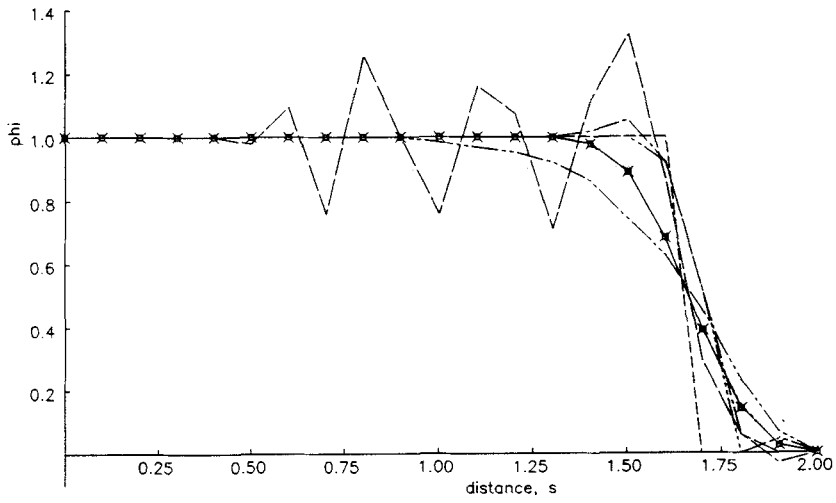


(c)

Figure 9. (Continued)

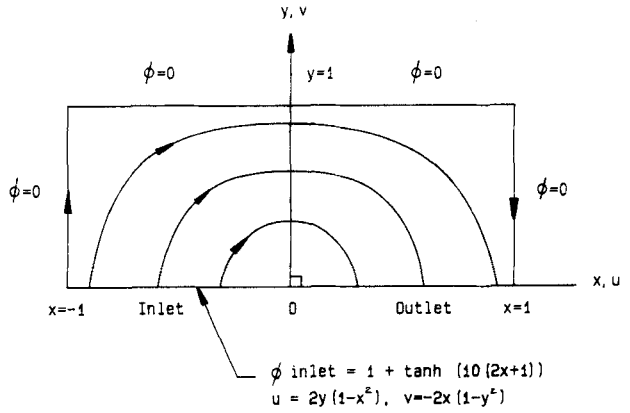


Figure 10. Smith and Hutton test case

$\theta = 22{\cdot}5°$, 45° and 67·5° respectively. The performance of MSU is very similar to that of the current formulation.

### 3.2. *Smith and Hutton test case*

This case was first proposed as a comparison exercise.[16] The flow domain together with the boundary conditions are shown in Figure 10 and illustrate two important features: (a) the streamlines show a large degree of curvature, which is a general feature of all recirculating flows; (b) the variation in $\phi$ at the inlet is highly non-linear, which may have resulted from the presence of a source or mixing of two streams at differing values of $\phi$.

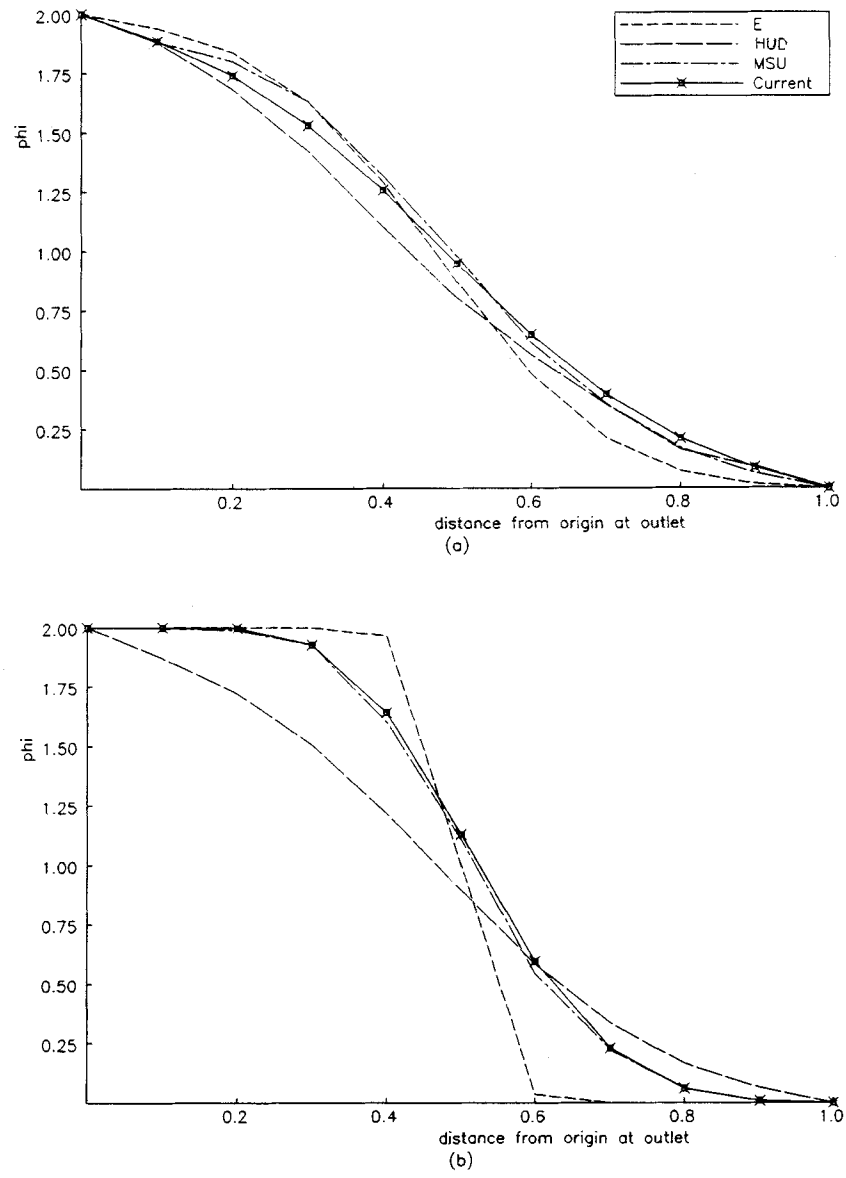


Figure 11. Comparison of results for Smith and Hutton test case: E, reference; HUD, hybrid upwind differencing; MSU, monotone streamline upwind;[11] $Pe$ = (a) 100, (b) $\infty$

The flow domain was divided into 11 rows and 21 columns, resulting in 231 equally spaced nodes and 400 elements. The present analysis was carried out for $Pe = 100$ and $\infty$. Figures 11(a) and 11(b) show the comparisons between the current results and those of previous workers against the reference solution provided in the Smith and Hutton comparison exercise.[16] Equation (16) is used to calculate the percentage false diffusion, with $\phi_{\text{reference}}$ used in place of $\phi_{\text{exact}}$. At $Pe = 100$ both the advection and diffusion mechanisms are effective as is seen from Figure 11(a). The current formulation shows the least false diffusion in the absence of spatial oscillation. The

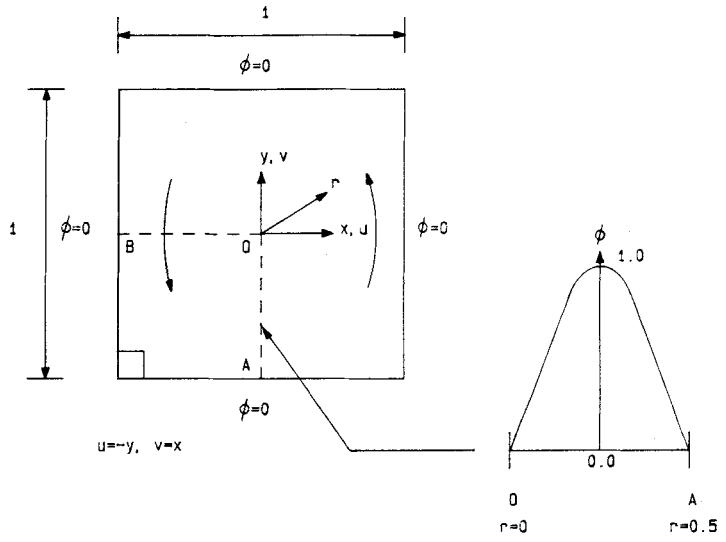


Figure 12. Rotating disk

present results compare well against the best of the past results, with a maximum of 9% false diffusion. Ideally, at $Pe = \infty$ the inlet profile must be carried undisturbed to the outlet plane. Figure 11(b) shows the outlet profile using the present formulation against those of other methods, exhibiting no spatial oscillations and a maximum numerical diffusion of 27%. MSU produces similar results to those of the present formulation.

### *3.3. Rotating disk*

The last test case modelled is that of pure advection transport in a rotating flow field cited in past publications.[8,12] The flow field and the boundary conditions are depicted in Figure 12; $\phi$ assumes a cosine variation along line OA. The exact solution to this problem is obtained by advecting the $\phi$-profile, along line OA, undisturbed around the square. In compliance with previous works,[8,12] the domain is subdivided into 31 equally spaced rows and columns, producing 961 nodes and 1800 elements.

Figure 13 compares the present results with the best of previously published results. SU2 shows no false diffusion and reproduces the exact solution. MSU has 11% false diffusion (equation (16)) and shows some degradation in the results at radial distances of 0·033 and 0·467 from the origin. The present formulation has a maximum of 9% false diffusion with degradation in computed $\phi$ at a radial distance of 0·467 from the origin.

## 4. CONCLUDING REMARKS

A new streamline upwind formulation using simplex elements has been presented. The upwinding is monotone and conservative and is shown to accurately capture the discontinuous nature of the advection phenomenon. The upwinding is discontinuous not only amongst the elements but also within each individual element, since only the downwind node receives the advection contribution. The formulation is equally applicable for all values of flow Peclet number. Its application to three stringent test cases shows that the formulation is free of all spatial oscillations and produces

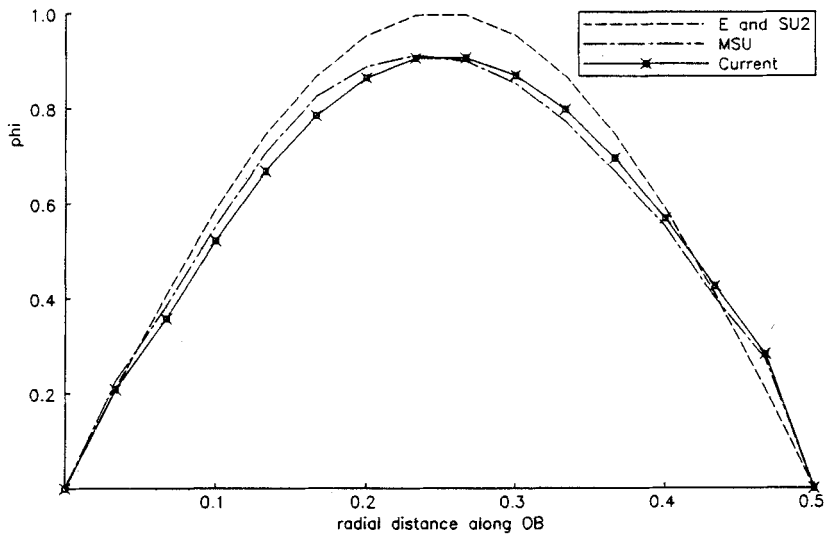


Figure 13. Comparison of $\phi$-profile along line OB: E, exact; SU2, streamline upwind;[8] MSU, monotone streamline upwind[11]

minimum levels of numerical diffusion, comparing well against the best of previous methods. For the case of advection skew to mesh and the Smith and Hutton test case the numerical diffusion is limited to the step discontinuity, where sharp changes in the imposed scalar field are present. This is in contrast to the QUICK scheme,[5] where the numerical diffusion is present along the outlet plane. The degree of numerical diffusion for these test cases is less than for most of the other techniques considered here. For the case of a rotating disk, SU2 reproduced the exact results whereas the current formulation exhibited some numerical diffusion. However, it must be noted that SU2 suffered from spatial oscillations in the first two test cases.

Diagonal dominance is always ensured by the current formulation so that any iterative solution technique could be used for solving the resulting system of linear equations. In particular, the novel fast iterative solver employed for this work was a variant of the TDMA procedure which was specifically adopted for the FEM.[23] The iterative solver only required the storage of the non-zero elements of the global coefficient matrix. Also, the solution sequence was unaffected by the global node and element numbering used to define the computational mesh. By sweeping along the direction of maximum change, fast convergence rates were obtained which reduced the computation times considerably.

The use of linear triangular elements allowed exact and efficient evaluation of the element integrals. This contrasts with the numerical integrations adopted by the finite element fraternity. Both the advection and diffusion calculations took on average 0·10 ms per element on a Digital VAX-8550 machine. By employing exact element integrations and iterative solution techniques, the overall finite element code required minimum computer storage and execution time. For example, the Smith and Hutton test case took 3·78 s to complete on the above machine. This was the collective time spent on mesh generation, matrix set-up and solution for both $Pe = 100$ and $\infty$ together. Since the present formulation uses the Galerkin element weighting function for the advection terms, it can be incorporated into any of the conventional Galerkin-type finite element codes.

ACKNOWLEDGEMENTS

The authors would like to acknowledge the Department of Mechanical Engineering, Nottingham Polytechnic, Nottingham, U.K. for funding the Research Assistantship to enable this work to be carried out and especially the Head of the Department and the Dean of the Faculty of Engineering, Professor B. L. Button, for his support.

REFERENCES

1. D. B. Spalding, 'A novel finite-difference formulation for differential expressions involving both first and second order derivatives', *Int. j. numer. methods eng.*, **4**, 551–559 (1972).
2. S. V. Patankar, *Numerical Heat Transfer and Fluid Flow*, Hemisphere/McGraw-Hill, New York, 1980.
3. H. S. Price, R. S. Varga and J. E. Warren, 'Application of oscillation matrices to diffusion-correction equations', *J. Math. Phys.*, **45**, 301–311 (1966).
4. M. Atias, M. Wolfshtein and M. Israeli, 'Efficiency of Navier–Stokes solvers', *AIAA J.* **15**, 263–266 (1977).
5. B. P. Leonard, 'A stable and accurate convective modeling procedure based on quadratic upstream interpolation', *Comput. Methods Appl. Mech. Eng.*, **19**, 59–98 (1979).
6. G. D. Raithby, 'Skew upwind differencing for problems involving fluid flow', *Comput. Methods Appl. Mech. Eng.*, **9**, 153–164 (1976).
7. M. A. Leschziner, 'Modeling turbulent recirculating flows by finite-volume methods—current status and future directions', *Int. J. Heat Fluid Flow*, **3**, 186–202 (1989).
8. T. J. R. Hughes and A. N. Brooks, 'A multi-dimensional upwind scheme with no crosswind diffusion', in T. J. R. Hughes (ed.), *Finite Element Methods for Convective Dominated Flows*, ASME, New York. 1979, pp. 19–35.
9. T. J. R. Hughes and A. N. Brooks, 'A theoretical framework for Petrov–Galerkin methods with discontinuous weighting functions: application to the streamline upwind procedure', in R. H. Gallagher, D. H. Norrie, J. T. Oden and O. C. Zienkiewicz (eds), *Finite Elements in Fluids, IV*, Wiley, London, 1982, pp. 46–65.
10. T. J. R. Hughes, M. Mallet, Y. Taki, T. Tezduyar, E. Tayfun and R. Zanutta, 'A one-dimensional shock capturing finite element method and multidimensional generalizations', *Proc. Workshop on Numerical Methods for Compressible Euler Equations*, INRIA, Rocquencourt, December 1983, pp. 371–408. SIAM, Philadelphia, PA, 1985.
11. J. G. Rice and R. J. Schnipke, 'A monotone streamline upwind finite element method for convection dominated flows', *Comput. Methods Appl. Mech. Eng.*, **48**, 313–327 (1985).
12. T. J. R. Hughes, M. Mallet and A. Mizukani, 'A new finite element formulation for computational fluid dynamics: beyond SUPG', *Comput. Methods Appl. Mech. Eng.*, **54**, 341–355 (1986).
13. T. J. R. Hughes and M. Mallet, 'A new finite element formulation for computational fluid dynamics: III. The generalized streamline operator for multidimensional advection-dominated systems', *Comput. Methods Appl. Mech. Eng.*, **58**, 305–328 (1986).
14. T. J. R. Hughes and M. Mallet, 'A new finite element formulation for computational fluid dynamics: IV. A discontinuity-capturing operator for multidimensional advective–diffusive systems', *Comput. Methods Appl. Mech. Eng.*, **58**, 329–336 (1986).
15. T. J. R. Hughes, L. P. Franca and M. Balestra, 'A new finite element formulation for computational fluid dynamics: V. Circumventing the Babuska–Brezzi condition: a stable Petrov–Galerkin formulation of the Stokes problem accommodating equal-order interpolations', *Comput. Methods Appl. Mech. Eng.*, **59**, 85–99 (1986).
16. R. M. Smith and A. G. Hutton, 'The numerical treatment of advection: a performance comparison of current methods', *Numer. Heat Transfer*, **5**, 439–461 (1982).
17. B. R. Baliga and S. V. Patankar, 'A new finite element formulation for convection–diffusion problems', *Numer. Heat Transfer*, **3**, 393–409 (1980).
18. O. C. Zienkiewicz, *The Finite Element Method*, 3rd edn, McGraw-Hill, New York, 1977.
19. T. J. R. Hughes and A. N. Brooks, 'Streamline upwind/Petrov–Galerkin formulation for convective dominated flows with particular emphasis on the incompressible Navier–Stokes equations', *Comput. Methods Appl. Mech. Eng.*, **32**, 199–259 (1982).
20. M. A. Leschziner, 'Practical evaluation of three finite difference schemes for the computation of steady-state recirculating flows', *Comput. Methods Appl. Mech. Eng.*, **23**, 293–312 (1980).
21. Y. A. Hassan, J. G. Rice and J. H. Kim, 'A stable mass-flow-weighted two-dimensional skew upwind scheme', *Numer. Heat Transfer*, **6**, 395–408 (1983).
22. T. J. R. Hughes, W. K. Liu and A. N. Brooks, 'Finite element analysis of incompressible viscous flows by the penalty function formulation', *J. Comput. Phys.*, **30**, 1–60 (1979).
23. F. Shemirani and K. Jambunathan, 'Regional alternating-direction implicit solver (RADIS)—a TDMA variant for completely unstructured grids generated by the FEM', to be published.